

Haverford College

Haverford Scholarship

Faculty Publications

Physics

1988

Stability boundaries and phase-space measurement for spatially extended dynamical systems

F. Simonelli

Jerry P. Gollub
Haverford College

Follow this and additional works at: https://scholarship.haverford.edu/physics_facpubs

Repository Citation

Simonelli, F., and Jerry P. Gollub. "Stability boundaries and phase-space measurement for spatially extended dynamical systems." *Review of scientific instruments* 59.2 (1988): 280-284.

This Journal Article is brought to you for free and open access by the Physics at Haverford Scholarship. It has been accepted for inclusion in Faculty Publications by an authorized administrator of Haverford Scholarship. For more information, please contact nmedeiro@haverford.edu.

Stability boundaries and phase space measurement for spatially extended dynamical systems

F. Simonelli and J. P. Gollub

Citation: *Rev. Sci. Instrum.* **59**, 280 (1988); doi: 10.1063/1.1140241

View online: <http://dx.doi.org/10.1063/1.1140241>

View Table of Contents: <http://rsi.aip.org/resource/1/RSINAK/v59/i2>

Published by the [American Institute of Physics](#).

Additional information on *Rev. Sci. Instrum.*

Journal Homepage: <http://rsi.aip.org>

Journal Information: http://rsi.aip.org/about/about_the_journal

Top downloads: http://rsi.aip.org/features/most_downloaded

Information for Authors: <http://rsi.aip.org/authors>

ADVERTISEMENT

physicstoday

Comment on any
Physics Today article.

Measured energy in Japan
David von Seggern
(dvseg@seismo.unr.edu) University of Nevada
July 2012, page 10
DIGITAL OBJECT IDENTIFIER
<http://dx.doi.org/10.1063/PT.3.1619>

Comment on this article
By the act of hitting a ball with a bat, one calculates the force energy to deliver the ball to its new location, but one must also take into account that the ball extended its energy release to that which became struck by the ball as its momentum ceased and passed energy to the struck team. Therefore the parameters of the damage extend into the future when the received energy to that pushed upon, later becomes released in a new event. Perhaps calculations of one added that in, while another's calculations did not. E.M.C.
Written by Edgar McCarvill, 14 July 2012 19:59

Stability boundaries and phase-space measurement for spatially extended dynamical systems

F. Simonelli and J. P. Gollub

Haverford College, Haverford, Pennsylvania 19041

(Received 5 August 1987; accepted for publication 9 October 1987)

Automated methods of studying the stability boundaries and phase-space dynamics of a spatially extended dynamical system are presented. The stability boundaries are determined accurately as a function of external parameters in an automated search. The amplitudes of the individual spatial modes are measured in real time in order to determine the structure of the attractors in phase space. Some control over initial conditions allows the basins of attraction and the transients leading to the attractors to be studied as well. The methods are applied specifically to interacting waves on a fluid surface, but should also be useful to other extended dynamical systems.

INTRODUCTION

Nonlinear dynamical systems are often studied by plotting trajectories traced out by the system in phase space. Even spatially extended dynamical systems, which in principle would seem to require a very high-dimensional phase space, can often be adequately described with only a few variables.¹⁻⁴ In some cases these variables can be identified with the normal modes of a related linear system, so that the amplitudes of those modes are the natural coordinates for a phase-space description.⁴⁻⁷ The dynamical behavior of the system is then studied by exploring the properties of the attractors, the limit sets toward which trajectories converge in the course of time. These attractors may be fixed points, limit cycles, tori, or strange (chaotic) attractors.⁸⁻¹⁰

Most of the experimental studies of extended dynamical systems have not attempted to carry out this program directly, because of the difficulty of actually measuring all of the significant dynamical variables. Instead, experimentalists have often attempted to characterize the dynamics by means of measurements of a single variable.¹¹⁻¹⁶ However, it is clear that this method, in which one attempts to construct a complete phase space trajectory from time-delayed versions of the measured variable,^{17,18} is limited in its ability to provide complete information on the dynamical evolution of spatial structures.

Several experimenters have attempted to measure a larger number of dynamical variables.^{4,19-22} Here we demonstrate a method that allows an essentially complete reconstruction of the phase-space dynamics and determination of stability boundary for spatially extended dynamical systems under favorable conditions. The method has the following advantages: (a) The coordinates of the phase space are the amplitudes of the linear normal modes of the system. (b) The structure of the parameter space which defines the domains of various types of dynamical behavior (fixed points, periodic states, etc.) can be determined in an automated fashion. (c) The method allows study of the transients and basins of attraction in addition to the attractors themselves. Although the methods have been developed to allow studies of parametrically excited waves on a fluid surface,^{4,6,7} and we

describe them in this context, they would, in part, be applicable to other types of spatially extended nonlinear systems.

I. EXPERIMENTAL SETUP

The basic design of an experiment for studying parametrically excited surface waves is shown in Fig. 1. The fluid container is a rectangular Plexiglas cell of typical horizontal dimensions between 5 and 10 cm. It is mechanically coupled to a large loudspeaker driven by an audio amplifier to provide a controllable vertical oscillation. The relevant external parameters of the system are the amplitude Δ and the angular frequency ω of the vertical oscillation. These need to be known with good accuracy and to be varied in an automated way. This goal is realized using a frequency synthesizer (HP model 3325A) that is computer controlled via a GPIB interface. In this way Δ and ω can be arbitrarily varied, and in addition, the phase ϕ can be suddenly changed, a feature that is very important for transient studies. The amplitude of the actual oscillation of the cell depends not only on the driving voltage, but also on other parameters such as the weight of the cell. Therefore, a separate system for measuring the amplitude of oscillation of the cell is required. The system we used is based on the deflection of a laser beam by a mirror attached to the cell. The translation of the laser beam is de-

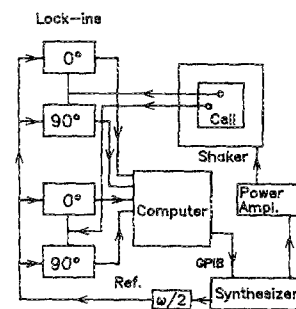


FIG. 1. Block diagram of the experiment. The computer sets the amplitude, frequency, and phase on a synthesizer via a GPIB interface. The resulting signal is applied to a shaker via an audio amplifier. Probes (photodiodes) detect the local light intensity on the screen due to refraction of the transmitted beam by the curved interface. The outputs of the probes are sent to lock-ins that detect the individual mode amplitudes.

tected by means of a position-sensitive photodetector. The amplitude of the oscillation of the photodetector's output gives, after calibration, the amplitude of the vertical motion of the cell. The accuracy of this method is about one part in 10^3 .

The desired dynamical information is contained in the surface deformation field of the waves. Various methods can be used to measure this field at isolated points, each one suitable for particular applications. The techniques described in the subsequent sections can be applied no matter what probe is selected. We use an optical system that has the main advantage of avoiding perturbations to the system (and the disadvantage of not being completely linear). A collimated white light beam (of horizontal dimensions comparable to the cell) enters the cell from the bottom and is refracted by the deformed free surface of the fluid. The fluid-air interface acts as an array of lenses that focus or defocus the beam, forming an image on a screen at the top of the cell.²³ If the wave height is small and the screen is close to the surface, the optical intensity on the screen is proportional to the Laplacian of the surface deformation.²³ In this approximation, the optical intensity field is easily related to the surface deformation field. Deviations from this approximation are discussed later in this paper.

For a rectangular geometry, the contribution to the surface displacement of each individual excited mode has the form⁴⁻⁷

$$Z_{mn}(x, y, t) = [A(t)\cos(\omega t/2) + B(t)\sin(\omega t/2)]F_{mn}(x, y), \quad (1)$$

where $F_{mn}(x, y) = \cos(k_m x)\cos(k_n y)$ gives the spatial structure of the linear modes of oscillation of the system, and $\omega/2$ is the angular frequency of the waves. (The wave oscillation occurs at half the driving frequency when Δ exceeds a frequency-dependent threshold.⁴⁻⁷) In this expression, the wave number of the mode is given by

$$k = (k_m^2 + k_n^2)^{1/2} = [(n\pi/L_x)^2 + (m\pi/L_y)^2]^{1/2}, \quad (2)$$

and m, n are integers used to label the modes. The functions $A(t)$ and $B(t)$ are mode amplitudes that, in the weakly nonlinear regime (not too far above threshold), vary on a time scale much longer than $1/\omega$.

The intensity distribution of light formed on the screen has the form

$$I(x, y, t) = (\text{const})Z_{mn}(x, y, t)k^2. \quad (3)$$

Therefore, the sensitivity of the measurement technique depends on the wave number, so that for comparable amplitudes, the modes with short wavelength are enhanced in the image; this can be taken into account after the modes are resolved. However, the wavelengths of the modes that interact are usually very close so that no correction is necessary in practice.

II. MEASUREMENT OF INDIVIDUAL MODE AMPLITUDES

The dynamical state of the system is specified by the slowly varying coefficients $A(t)$ and $B(t)$ of each of the spa-

tial modes. Therefore, a measurement technique is desired that gives those coefficients in real time with minimal handling of information. For this reason, we avoid the brute force method of digitizing and Fourier transforming the entire optical image.

If a single mode is excited, the spatial distribution is known. By placing a single photodiode in a suitable position (for example at a point where the oscillation is maximum) and connecting the photodiode output to a two-phase lock-in amplifier, $A(t)$ and $B(t)$ are obtained in real time and with a considerable noise reduction. When N modes are present, it is sufficient to use a number of photodiodes equal to N . The amplitudes of the modes can be easily resolved because both the positions of the photodiodes and the spatial dependence of the excited modes are known. The calculation only requires the inversion of a $2N \times 2N$ matrix at each time step. The method is practical if N is relatively small, and in that case, the calculation is very simple and can be performed with any microcomputer system. Noise in the measurement process itself turns out to be insignificant, given proper attention to stability of the light source. The typical signal-to-noise ratio is about 10^3 .

There are, however, several limitations to the accuracy of this mode decomposition process. The primary ones are (a) neglected modes and (b) optical nonlinearity.

(a) Neglected modes: There is always some component of oscillation of the surface at the same frequency ω of the driving signal (in addition to the dominant motion at angular frequency $\omega/2$). These are generated primarily by boundary effects. The amplitudes of these higher frequency modes are small in comparison to the modes of interest, but they are enhanced in the optical intensity by the k^2 factor [see Eq. (3)]. The lock-ins filter out most of that signal, but some remains, and appears as noise on the measured amplitudes. (Of course, in some cases, these higher modes can also influence the subharmonic modes through hydrodynamic nonlinear interactions.) As a result, the minimum surface wave amplitude that can be distinguished from the background noise is typically 0.1% of the wavelength.

(b) Optical nonlinearity: Nonlinearity in the optical imaging system gives an additional and potentially serious limitation on the accuracy of measurement. If the wave height is not small in comparison to the wavelength, or if the screen is too far from the surface, then the optical intensity field is nonlinear in the mode amplitudes. In addition, it is nonlocal (the intensity at a point on the scene depends on the surface deformation over an extended area²³). In the worst case encountered, the wave amplitude was 20% of the wavelength, and numerical computations show that the measured amplitude in that case is in error by about 25%.

If desired, this effect can be eliminated by a calibration based on numerical computation or on the use of a different probe. However, some nonlinearity is tolerable, since very often one seeks primarily to resolve qualitative features such as the presence or absence of certain modes, the nature of the time dependence, or the dimension of the attractors and their symmetry properties. We typically do not bother to make the correction.

(c) Cross talk: There is also a small amount of spurious

cross talk between the mode amplitudes, but this is found empirically to be only about 2% in typical cases.

In conclusion, the optical probes are satisfactory, but others can be substituted if a more linear response is desired and the resulting perturbations can be tolerated. The subsequent discussion would not be affected by the transducer used to obtain the mode amplitudes.

III. MEASUREMENT OF STABILITY BOUNDARIES IN PARAMETER SPACE

A. Time-independent threshold

The first step in investigating the system is the scanning of frequency and amplitude in order to find the stability boundary of the flat surface. The process of finding the threshold of an instability can be quite time consuming, since the time scale of the evolution diverges at the critical point. If the nature of the instability is known, a theoretical model can, in principle, be used to obtain the threshold by fitting the results of measurements performed at some distance from the threshold. In a general case, however, accurate theoretical models are not available, in part because secondary instabilities can give complicated behavior close to the threshold.

We used a general approach that does not presume any theoretical model. The method turns out to be very useful for surface waves where the nature of the instability depends on the frequency of excitation. In what follows we give first a qualitative description of the automated process and subsequently address some more detailed aspects.

At each frequency the driving amplitude Δ is increased from zero in large steps. For every step, after a conveniently selected waiting time T_w , the outputs of the lock-ins are recorded, and the averages and derivatives of the signals are computed and compared to threshold values. When the system is found to be above threshold, the value of Δ recorded is the first approximation of the threshold Δ_+ . Then Δ is decreased with a reduced average rate R (step size δ divided by T_w). In this way the value of Δ at which the surface becomes flat again is detected (first approximation of Δ_-). At that point R is further reduced and Δ is increased again in order to find Δ_+ with higher precision. The entire process is repeated until the maximum accuracy allowed by the system is attained.

Some points are worth noting in this procedure:

(a) The derivative of the signal is used together with the signal itself to detect the instability. This is done because in some cases the instability can be detected earlier using the derivative. When decreasing Δ , the derivative is measured with the purpose of adjusting the waiting time accordingly. As a consequence the efficiency is improved.

(b) A method of successive approximation is more efficient than a single search using small steps because one avoids spending long times at values of Δ far from Δ_- and Δ_+ . The particular choice of R and of the factor ρ by which R is divided at each reversal of direction is the result of a trade off between various sources of inefficiency: excessive number of reversals of direction if ρ is too low; excessive

TABLE I. Successive approximations to Δ_- and Δ_+ during the process of threshold search. The convergence to the final values is clearly evident. Here δ is the amplitude of steps, δ_0 is the smallest step used, and T_w is the waiting time in the first stage of the search. No hysteresis is found at this particular frequency.

Step size δ/δ_0	Waiting time T_w/T_{w_0}	Approximation to (μm)	
		Δ_+	Δ_-
32	1	174.1	
16	1		149.1
8	1	166.5	
4	1		154.0
2	1	161.8	
1	1		159.5
1	10	160.3	
1	10		159.8

overshoot when R is too high; and the possible presence of hysteresis.

We did not attempt an analytical optimization, and the method we use is based on experience. The threshold search has two stages. In the first stage, T_w is held constant while δ is divided by two at each reversal. The time T_w is selected in such a way to allow an almost complete relaxation of the wave amplitude (more than 50% of the final value) when $\Delta = \Delta_+ + \delta$ for the biggest δ (some trials are required to find the appropriate time for the system under study). This is a good compromise that achieves a reasonable increase of accuracy at each reversal while controlling the waste of time due to overshoots and to hysteresis ($\Delta_+ \neq \Delta_-$). In the second stage, the search for Δ_+ and Δ_- continue separately and T_w is increased by a factor of 10 or more in order to allow a more complete relaxation at the smallest δ .

A typical time for obtaining the two thresholds at one frequency for our system is 10^4 s. The accuracy is typically 0.3%, and the reproducibility is of the same order. An example of the successive approximations to Δ_- and Δ_+ found during the search process at a particular frequency is shown in Table I.

The entire search is automatically repeated for several frequencies in the desired range. The graph in Fig. 2 is an example of Δ_- and Δ_+ as a function of the driving frequen-

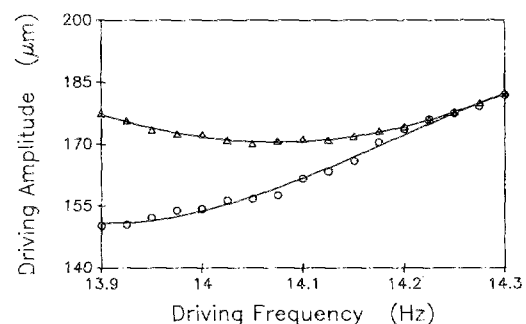


FIG. 2. Stability boundary (for increasing and decreasing driving amplitude) for a pair of degenerate modes (mode $m = 3$, $n = 2$, and mode $m = 2$, $n = 3$) in a square cell of size 6.2 cm. The circles are the decreasing threshold values Δ_- , while the triangles are the increasing values Δ_+ . The abscissa is the driving frequency $\omega/2\pi$.

cy $\omega/2\pi$. These curves constitute stability boundaries of the system.

B. Threshold of time dependence

The same program structure described above is used when investigating the boundaries of the regions of time dependence, in which the asymptotic mode amplitudes depend on time. In this case, instead of using the average and derivative of the signals to characterize the status of the system, we use the average and standard deviation. The boundaries of the time-dependent regions can be obtained with the method of successive approximation that we described in Sec. III A for the time-independent threshold search. The boundaries in parameter space of various types of dynamical behavior (such as stable superpositions of several modes) can also be found in the same way. All the information is then combined to draw a detailed diagram of the parameter space.

IV. RECONSTRUCTION OF THE PHASE SPACE

Experiments on dynamical systems generally emphasize the study of asymptotic behavior,^{1-4,11-16,19-22} but it is also of interest to know about unstable solutions, basins of attraction (the basin of attraction of an attractor is the set of initial conditions that lead asymptotically to the attractor itself), and the transient behavior.²⁴⁻²⁶

The method we describe for experimental investigation of the phase space has been used in numerical studies,²⁴⁻²⁶ but its application to physical systems requires a mechanism for controlling the initial conditions. The initial condition is specified by the amplitudes A and B , in Eq. (1), for all of the interacting modes. Those amplitudes cannot be controlled directly but can be varied indirectly by means of changes in the driving parameters Δ and ω .

If the system is being analyzed at the point (Δ_0, ω_0) , it is first prepared at another point (Δ_1, ω_1) . A good variety of initial conditions is usually obtained by selecting the various points (Δ_1, ω_1) along several circles (in parameter space)

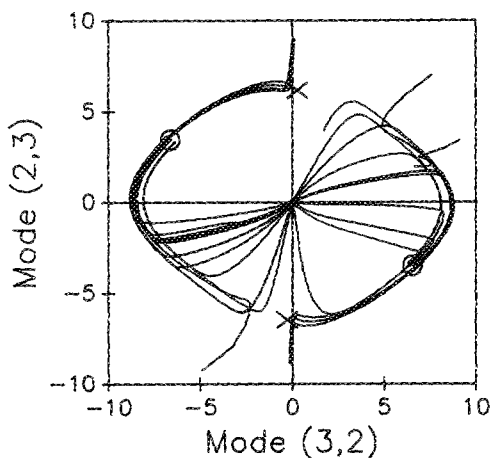


FIG. 3. Transients in a bidimensional projection of the four-dimensional phase space for the modes $m = 3, n = 2$ and $m = 2, n = 3$. Here $\omega/2\pi = 14$ Hz and $\Delta = 200 \mu\text{m}$. Two stable fixed points (superpositions of the two modes) are easily seen (circles). Two saddles, a particular type of unstable fixed point, are located on the separatrix of the basins of attraction of the two stable fixed points and are indicated by crosses.

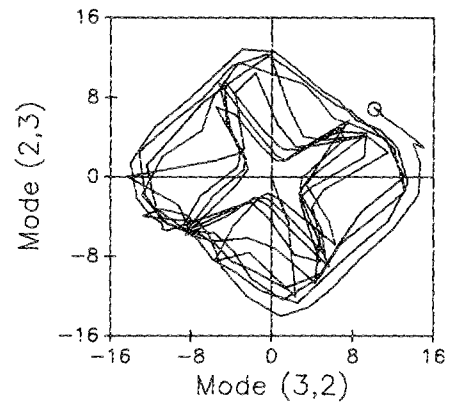


FIG. 4. Bidimensional projection of a complicated transient that leads to a fixed point (circle). This complexity would be missed in a study of the asymptotic behavior.

with center (Δ_0, ω_0) and various radii. Sudden changes in the phase ϕ of the driving signal are also used when it is important to change the ratio of A and B [see Eq. (1)].

In Fig. 3 we illustrate this systematic variation in initial conditions by displaying 32 resulting transient trajectories in a bidimensional projection from the four-dimensional phase space. The projection is obtained by measuring each of the two-mode amplitudes at given phases with respect to the driving signal. (The phases are measured in the steady state.) Two fixed points corresponding to mixed modes (stable superpositions) are easily seen. Two saddle points (unstable fixed points) can also be detected on the separatrix of the basins of attraction of the two stable fixed points. In this case the basins of attraction can be easily approximated even with a limited number of transients, but sometimes a larger number is required. The saddle points would be overlooked by a study limited to the asymptotic behavior.

Another example of the utility of studying transient behavior is shown in Fig. 4, where we show a complicated transient that leads to a fixed point. Even though the asymptotic solutions are similar in this case and in that of Fig. 3, the transients show that the phase-space structure is very different in the two experiments.

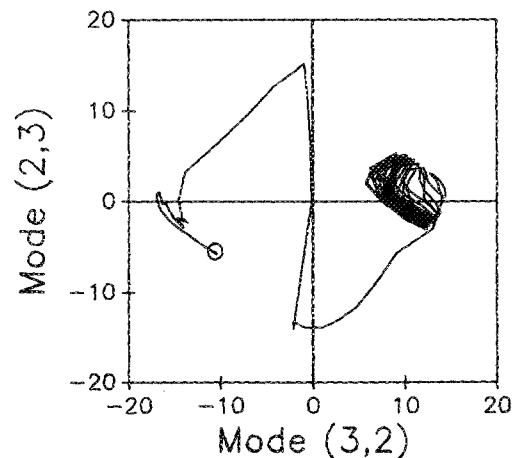


FIG. 5. Various attractors can be present for the same values of the external parameters. In this case a fixed point (circle) and a limit cycle are reached for slightly different initial conditions.

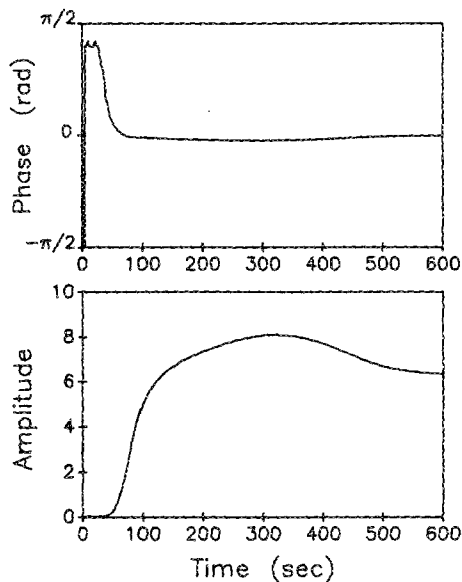


FIG. 6. Phase and amplitude of one of the modes $m = 3, n = 2$, as a function of time. Referring to Eq. (1), the phase is defined as $\arctan(B/A)$ and the amplitude as $(A^2 + B^2)^{1/2}$. It is easily seen that the phase relaxes much more quickly than the amplitude does.

In some cases, various distinct types of attractors can coexist for the same values of Δ and ω . In Fig. 5 we show a bidimensional projection of the four-dimensional phase space where a fixed point coexists with a limit cycle. The two different types of attractors are reached for different initial conditions close to the origin. In this case, a small initial difference gives a completely different asymptotic behavior.

It is also useful to look at the transient behavior in the time domain, in order to distinguish the time constants associated with different variables. We present an example in Fig. 6, where it may be seen that the phase of a mode amplitude (with respect to the driving signal) relaxes much more quickly to its final value than does the amplitude itself.

V. DISCUSSION

The methods presented in this paper for studying stability boundaries and phase-space dynamics for extended dynamical systems are based on the possibility of resolving spatial mode amplitudes in real time using local probes. The various regions in parameter space and types of phase-space dynamics can then be associated with particular spatial structures and their time evolution. These methods can be

applied to other spatially extended systems, provided that the number of spatial modes involved is relatively small (perhaps up to 10), and each mode is coherent over the size of the system. If this is not true, as might occur in systems that are much larger than the basic spatial wavelength, then a decomposition into global mode amplitudes might not be useful.²⁷

The sample results shown here are illustrative and their use to study the structure of the phase space for interacting surface waves will be presented elsewhere.

ACKNOWLEDGMENTS

This work was supported by DARPA-URI Contract to Princeton University and earlier by National Science Foundation Grant No. MSM-8310933.

- ¹H. Swinney and J. P. Gollub, *Physica (Utrecht)* **18D**, 448 (1986).
- ²B. Malraison, P. Atten, P. Bergé, and M. Dubois, *J. Phys. Lett.* **44**, L-897 (1983).
- ³A. Brandstater and H. Swinney, *Phys. Rev. A* **35**, 2207 (1987).
- ⁴S. Ciliberto and J. P. Gollub, *J. Fluid Mech.* **158**, 381 (1985).
- ⁵T. B. Benjamin and F. Ursell, *Proc. R. Soc. London Ser. A* **225**, 505 (1954).
- ⁶E. Meron and I. Procaccia, *Phys. Rev. Lett.* **56**, 1323 (1986).
- ⁷E. Meron, *Phys. Rev. A* **35**, 4892 (1987).
- ⁸*Hydrodynamic Instabilities and the Transition to Turbulence*, edited by H. L. Swinney and J. P. Gollub (Springer, New York, 1981).
- ⁹P. Bergé, Y. Pomeau, and C. Vidal, *Order Within Chaos* (Wiley, New York, 1984).
- ¹⁰J. Guckenheimer and P. Holmes, *Nonlinear Oscillations, Dynamical Systems, and Bifurcations of Vector Fields* (Springer, New York, 1983).
- ¹¹J. P. Gollub and H. L. Swinney, *Phys. Rev. Lett.* **35**, 927 (1975).
- ¹²J. P. Gollub and S. V. Benson, *J. Fluid Mech.* **100**, 449 (1980).
- ¹³A. P. Fein, M. S. Heutmaker, and J. P. Gollub, *Phys. Scr.* **T9**, 79 (1985).
- ¹⁴M. Giglio, S. Musazzi, and U. Perini, *Phys. Rev. Lett.* **53**, 240 (1984).
- ¹⁵J. Stevans, F. Heslot, and A. Libchaber, *Phys. Rev. Lett.* **55**, 596 (1985).
- ¹⁶M. Dubois, M. A. Rubio, and P. Bergé, *Phys. Rev. Lett.* **51**, 1446 (1983).
- ¹⁷N. H. Packard, J. P. Crutchfield, J. D. Farmer, and R. Shaw, *Phys. Rev. Lett.* **45**, 712 (1980).
- ¹⁸F. Takens, in *Lectures Notes in Mathematics 898*, edited by D. A. Rand and L. S. Young (Springer, Berlin, 1981).
- ¹⁹M. S. Heutmaker, P. N. Fraenkel, and J. P. Gollub, *Phys. Rev. Lett.* **54**, 1369 (1985).
- ²⁰S. Ciliberto and F. Simonelli, *Europhys. Lett.* **2**, 285 (1986).
- ²¹M. Gorman, P. J. Widmann, and K. A. Robbins, *Physica (Utrecht)* **19D**, 225 (1986).
- ²²M. Funakoshi and S. Inoue, *Phys. Lett. A* **121**, 229 (1987).
- ²³M. Born and E. Wolf, *Principles of Optics* (Pergamon, New York, 1980).
- ²⁴F. T. Arecchi, R. Badii, and A. Politi, *Phys. Rev. A* **32**, 402 (1985).
- ²⁵F. C. Moon and G. X. Li, *Phys. Rev. Lett.* **55**, 1439 (1985).
- ²⁶C. Grebogi, E. Ott, and J. A. Yorke, *Phys. Rev. Lett.* **56**, 1011 (1986).
- ²⁷T. Bohr, G. Grinstein, Yu He, and C. Jayaprakash, *Phys. Rev. Lett.* **58**, 2155 (1987).